AIDA: Measuring Asteroid Binary System Parameters and DART-Imparted Deflection using the AIM Spacecraft

By Julie BELLEROSE,[1)] Shyamkumar BHASKARAN,[1)] and Steven CHESLEY[1)]

[1)]*California Institute of Technology, Jet Propulsion Laboratory, Pasadena, USA*

(Received June 21st, 2017)

The Asteroid Impact and Deflection Assessment (AIDA) mission concept would demonstrate an asteroid deflection through a high velocity spacecraft impact on the moon of the binary asteroid system Didymos. The NASA DART spacecraft would be launched on an impacting trajectory, while the ESA AIM spacecraft would be orbiting and observing the system before and after the impact. Radio science measurements with AIM provides information on the complex dynamics of the binary system. Combined with the DART experiment, the ability to measure the imparted ΔV has significant implications for how well the proposed AIDA mission would serve as a deflection demonstration. In addition, the impact-induced deflection, cratering, and mass transfer can be interpreted as indicators of surface properties. We provided preliminary analyses of the measurability of the DART impact as function of generic AIM spacecraft proximity operations and knowledge of the Didymos system from radio science techniques.

Key Words: AIDA, radio science, binary asteroid

1. The AIDA Mission Concept

The AIDA mission is a proposed international collaboration between ESA and NASA to demonstrate and measure the effects of a kinetic impact on a small asteroid. The mission target is the binary near-Earth asteroid (65803) Didymos, which consists of a 775 m (+/-10%) diameter primary body, and a 163 m (+/-0.018 m) diameter secondary body orbiting 1.18 km +/- 0.04 km away from the system barycenter. The mission concept involves two mutually independent spacecraft: an orbiter and an impactor.

The ESA-led orbiter, the Asteroid Impact Mission (AIM), is intended to launch in October 2020 and arrive at Didymos in the Spring 2022. Its goals are both science and technology demonstration as it would characterize the system prior to impact, and measure the deflection. The science focus is on the smaller body of the asteroid system, with the spacecraft performing high-resolution visual, thermal and radar mapping to build detailed maps of its surface and interior structure [1,2].

The NASA-led Double Asteroid Redirection Test mission (DART) would arrive at Didymos in late 2022 and impact the moon at approximately 6 km/s. The change imparted in the mutual orbit rate, estimated to less than 1%, would be measured by Earth-based telescopes [3,4]. AIM would perform detailed before-and-after impact comparisons. Figure 1 illustrates the mission concept. The next sections detail covariance analysis performed with the AIM spacecraft.

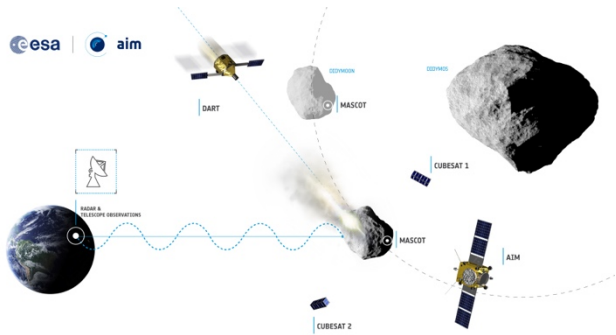

Fig. 1. AIDA mission concept.

2. Background: Radio Science at Small Bodies, and connection to Asteroid Deflection

Radio science at small bodies is not new. To date, three spacecraft have been in proximity of either an asteroid or a comet.

The NEAR-Shoemaker spacecraft spent about one year at Eros, a 33-km by 13-km asteroid. In the last 6 months of the mission, NEAR stayed in orbit at an altitude below 50 km, and in a 35-km circular orbit in the last 2 months for precise estimations of Eros' physical parameters. It landed on Eros in February 2001, where the spacecraft was operated for an additional two weeks. Its GM (mass times gravitational constant), pole orientation and rotation state were determined to less than 0.1% accuracy, with its gravity field also estimated to degree and order 24 [5,6].

The Hayabusa mission visited a much smaller asteroid, Itokawa, for a few months in 2005. It was the first spacecraft to touch

the surface and come back with samples. The spacecraft returned to Earth in 2010. The science team was able to get a refined estimate of Itokawa's mass by having the spacecraft come as close to 5 km from the surface without using thrusters. Itokawa's mass was estimated with an error of 5-6%, and its gravity field to degree and order 4 [7,8].

Then, just last year, the Rosetta spacecraft ended an incredible journey at the comet Churyunov-Gerasimenko (C-G). After rendezvous'ing with C-G in 2014 and releasing its lander, Philae, the spacecraft orbited the comet for 2 years. In the summer 2016, the ESA flight dynamics team started lowering the spacecraft orbiting altitudes, getting invaluable data on the comet physical parameters. From its proximity operations, C-G's mass, pole orientation, and ephemeris were estimated with errors less than 0.1% [9,10].

The Asteroid Impact and Deflection Assessment (AIDA) mission would bring an additional dimension to this interesting problem… How do we do radio science at a binary? What sort of approaches can provide sufficient information to refine the system uncertainties and allow measurement of an asteroid impact? Not much work has looked at this particular problem, and even less in the context, and to specific measurement requirements, of an asteroid deflection mission through high velocity impact.

3. Radio Science at a Binary: Problem Definition

There has been a number of studies on the dynamics of binary systems. The problem is complex as both the rotational and translational dynamics are coupled. The Full Two Body Problem describes the dynamics of the binary itself, whereas the Restricted Full Three Body Problem can be used to model the dynamics of a spacecraft, or point mass, in the system vicinity. There exists levels of simplifications in the formulation of the mutual potential to design orbits and compute regions of stability, and to speed up the computations while keeping interesting dynamical behavior [11].

For this study, we chose to propagate the dynamics of the Didymos system, along with the AIM spacecraft, as an n-body problem accounting for all planetary perturbations, with solar radiation pressure and other typical non-gravitational forces. The radio science and uncertainty analysis was performed using the JPL navigational software, MONTE, which is currently used in all navigation flight operations [12]. The Didymos ephemeris, along with its associated error estimate, were provided by the Solar System Dynamics (SSD) Group at JPL. The ephemeris of Dydimos is also available through the JPL Horizons website [13]. The primary and secondary bodies of the system, designates as "Didymain" and "Didymoon", respectively, were then defined as bodies orbiting around their mutual barycenter, Didymos. We assumed a density of 2146 kg/m^3 for both bodies. The Didymain and Didymoon orbits were integrated using initial conditions from higher fidelity simulation of the Didymos system provided by the SSD Group, which accounts for full shape modeling and coupling of the system [14]. The Dydimos system parameter values and associated *a priori* uncertainties on asteroid masses and states were taken from the AIDA reference document [15]. The bodies' harmonics apriori uncertainties were assumed using techniques developed by McMahon et al, presented at LPSC in 2016 [16]. The spacecraft was modeled as a point mass, and we assumed momentum wheel desaturations occurring every two days (with associated *a priori* uncertainties of 1mm/s in the Delta-V), and compared with a "clean" spacecraft. Table 1 lists the *a priori* uncertainties used for the radio science study.

Table 1: Didymos parameters and 1-sigma *a priori* errors.

Parameters	**Values**	**1-sigma**
Didymain states	Defined at Epoch	0.5km; 0.01km/s
moon states	Defined at Epoch	0.5km; 0.01km/s
AIM spacecraft	Approach specific	0.05km; 0.005km/s
SRP factor	1	100%
Harmonics factor	1	100%
Pole (RA and DEC)	310 deg, -84 deg	20 deg; 5 deg
Spin state	2.26 hrs	0.0001 hr

We simulated raw observables, in terms of Doppler, Range, and optical measurements using MONTE's simulation toolbox. The data simulated included radiometric measurements for seven 8-hr tracks per week, over X-band frequency. The study also used optical measurements using a 13 deg field of view (FOV) (wide angle camera, WAC, 110 μrad instantaneous FOV (IFOV)) and a 5 deg field of view camera (narrow angle, NAC, 85 μrad IFOV). Optical picture were alternated between the main and the moon bodies every six hours, with equally generated landmarks on each bodies. Note that the pointing uncertainty was not included and is left as future work.

The study first looked at typical proximity approaches to get the evolution of the system uncertainties within the operational environment described above.

4. Proximity Operational Approach Strategies

Since AIM is planned to arrive about 6 months before the DART-impact experiment, it would be able to gather a variety images from the system. During this time, a shape model would be built as the spacecraft gets closer to the system, and surface landmarks can then be used for close-up navigation. This study assumes a preliminary shape model has been made available from a remote observation campaign, and is used to augment the radio science experiment.

Terminator orbits and slow flybys to either bodies are the likely approach strategies to be adopted after an initial remote observation campaign; terminator orbits can be shown to be stable, and flybys provide impact free trajectories.

Figures 2 and 3 show terminator orbits with orbit radius of 2 km and 5 km, respectively. Those orbits are called terminator as the spacecraft orbit lies in a plane perpendicular to the sun-line, or in other words, in a plane parallel to the asteroid terminator plane where the surface transitions from light to dark. Due to the solar radiation pressure acting on the spacecraft, the orbit would precess at the same rate as the asteroid orbits about the Sun. Here, they were propagated for 12 days. Note that due to the size of the main body, the 5 km orbit is about the most distant feasible orbit. Further than 5 km, solar radiation pressure destabilizes the orbit, and only partial arcs of 4-5 days can be achieved without requiring maintenance maneuvers. The 2 km orbit in figure 3 shows much more stable operations. With the secondary asteroid orbiting at 1.18 km from the barycenter, this gives about 800 m clearance between the spacecraft and the moon at closest approach. Figures 4 and 5 show the distance between the spacecraft and either the main or the moon asteroid during those 12 days, respectively.

For those orbits, no maintenance maneuvers are required. However, the simulations accounted for errors in performing momentum wheel management maneuvers, referred to as desaturations maneuvers. Those errors are accounted for in the covariance analysis presented next.

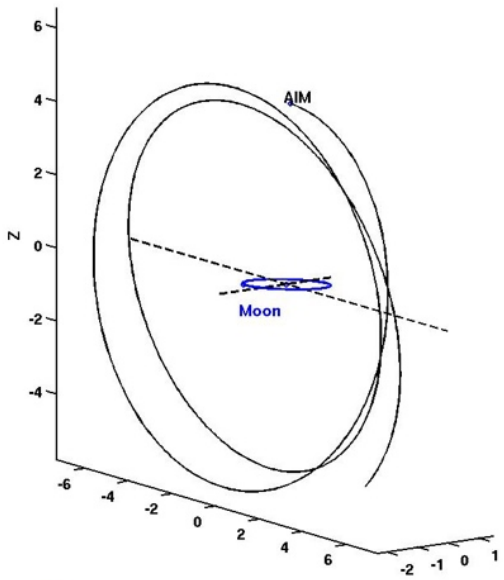

Fig. 2. 5 km terminator orbit.

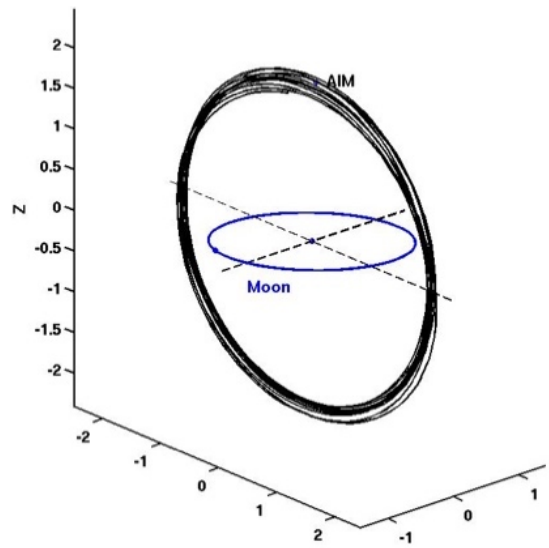

Fig. 3. 2km terminator orbit.

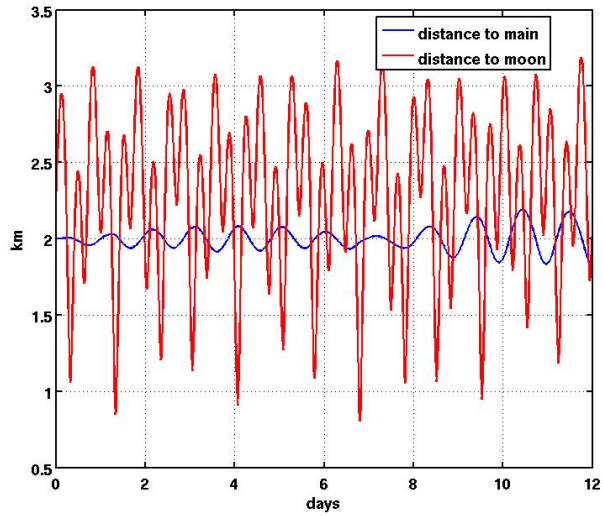

Fig. 4. Range plot for the 2 km orbit case.

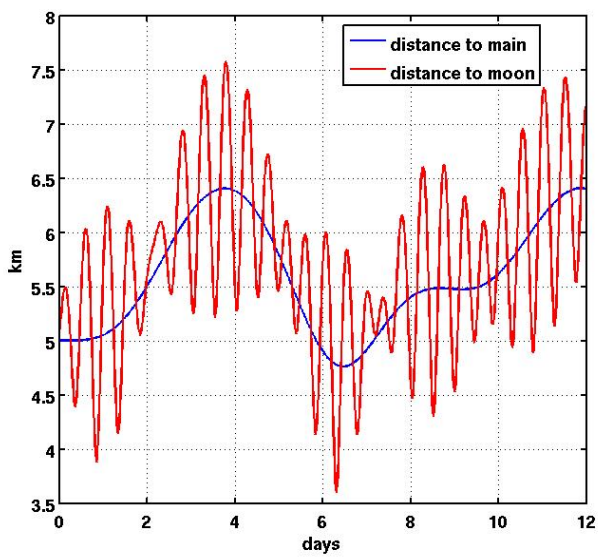

Fig. 5. Range plot for the 5 km orbit case.

The slow hyperbolic flyby approach is a fail-safe strategy and can take advantage of operations involving release of surface probes like the MASCOT-2 currently proposed as payload on AIM. Since the probe release would involve minimal trajectory correction maneuvers after the initial trajectory injection, we looked at the ideal situation where the radio science team would be able to obtain Doppler, range and optical measurements through the approach. Figures 6 and 7 show two flybys, one of the main body, at 1500 m distance during its closest approach where the moon is located at its furthest location on its orbit from the close approach, and the other of the moon, at 300 m altitude. Those simulations assumed injection into the proper hyperbolic trajectory from a 10 km distance, with a close approach 24 hours later. The corresponding distance plots, showing ranges between the spacecraft and either the main or the moon bodies, are show in Figures 8 and 9, respectively.

With the simulated data described earlier, those two types of approaches (the terminator orbits and slow hyperbolic flybys) include one radiometric tracking pass of 8 hours per day, and pictures of asteroid landmarks every 6 hours. We compared the exact same trajectories and error calculations with and without the optical navigation images in the next section.

MONTE has a detailed model for the solar radiation pressure acting on a given spacecraft. Although modeled as a point mass, we defined a flat plate with $10m^2$ surface area to account for this non-gravitational force.

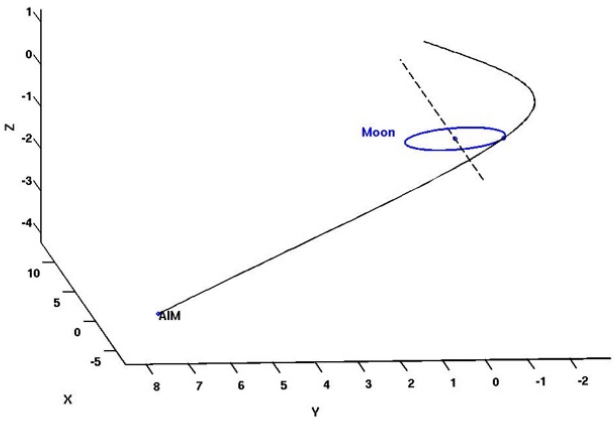

Fig. 6. Slow hyperbolic flyby of Didymoon, 300 m at close approach.

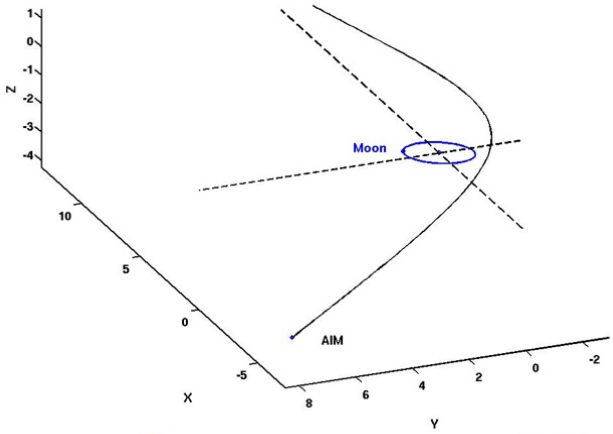

Fig. 7. Slow hyperbolic flyby of Didymain, 1500 m at close approach.

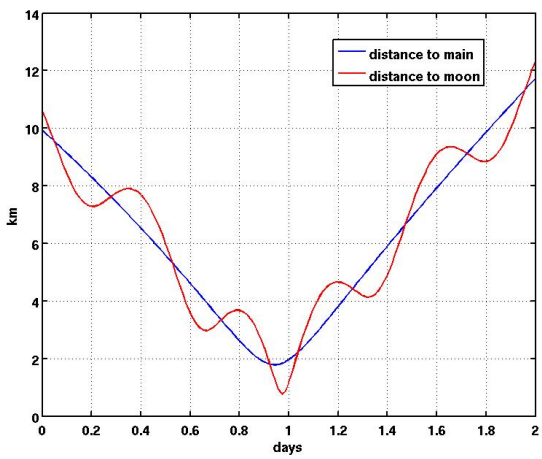

Fig. 8. Range plot for Didymoon flyby.

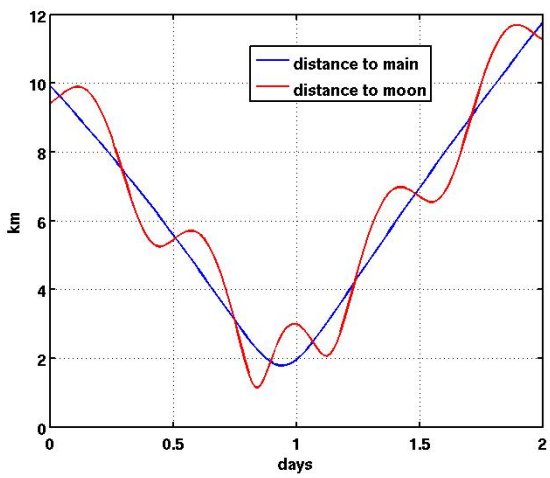

Fig. 9. Range plot for Didymain flyby.

4. Covariance Results for the Didymos System

In order to have visibility on the impact and quantifying the measurability of the DV, the Didymos system needs to be determined to lower uncertainties. The error contribution for the Didymos system states, the spacecraft states, the harmonics and pole parameters, and zero-mean stochastic accelerations are estimated via a linearized least-square estimation process in MONTE. The *a priori* values of these parameters are constrained using values listed in Table 1. To emulate operation conditions, the error contribution associated with the sensitivity to modeling the planetary ephemeris, Earth platform parameters, and media calibrations are also included in the filter. Because those parameters are not estimated but the error is accounted for, they are referred to as consider parameters.

For each of the orbits mentioned in the previous section, we recorded the errors of the estimated parameters mentioned above. The bodies' GM are of special interest as they indicate the degree to which we can measure the dynamics of the system, and thus directly linked to measuring an impact that would disturb the system mutual orbit. Figure 10 shows the percentage uncertainty, i.e. post-fit sigma over the apriori sigma, with respect to the terminator orbit altitude. One can clearly see the advantage of using optical navigation (13 deg FOV), especially for measuring the moon's GM. On the figure, the green and purple curves represent the GM uncertainties of Didymoon and Dodymain when including optical navigation images, respectively. Both indicate a much lower uncertainty compared to without optical images (blue and red). For the main body, the GM uncertainty gets reduced greatly from radio tracking alone, getting below 10% when orbiting at 25 km. The addition of optical navigation reduces the GM further, to below 1% for orbits within 10 km of the system. Radio tracking alone does not help determining the moon itself. However, with optical data, the moon's GM uncertainty reduces to 20% for orbiting altitude of 5 km and less, and to single digit percentage when below 4.5 km in altitude. Note that the use of the narrow angle camera (5 deg FOV) reduces the number of landmarks obtained, resulting in GM uncertainties one order of magnitude larger. Since the impact is to happen on the moon, it is especially important to reduce the moon's GM uncertainty.

5. DART Impact Observation

The deflection demonstration of the AIDA mission involves the DART spacecraft impacting Didymoon as 6 km/s. The effect this impact would have on the moon is estimated to be around 0.4 mm/s in magnitude. It is thus necessary to measure the impact Delta-V remotely to well within 0.4 mm/s, in radial and along track components in particular.

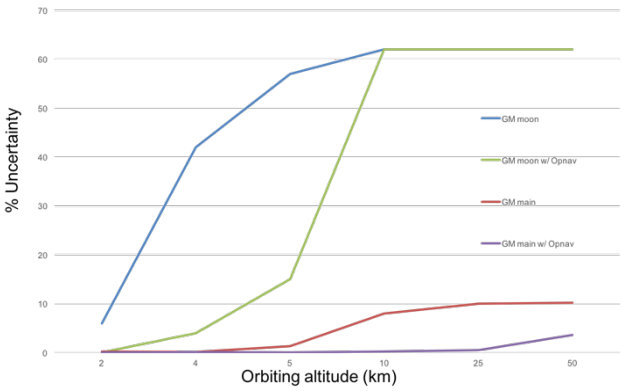

Fig. 10. Main and moon's GM uncertainties as function of orbit altitude, with and without optical navigation (13 deg FOV).

The Didymos system current knowledge has too large *a priori* uncertainties to allow any visibility on the DART impact. Realistically, the radio science acitivities presented in previous sections would provide enough data to reduce the system uncertainties, so they can subsequently be used for remote observation of the impact. Hence, for this study, we updated the system a priori uncertainties with those obtained from the 2 km terminator orbit case and added a scale factor of 5 for conservatism. The impact was modeled as an impulse burn on Didymoon with a 1-σ uncertainty of 1 mm/s, and added to the estimated parameter list. The uncertainties from planetary ephemerides, and from other Earth parameters are still accounted for as previously described.

As a worst case observation scenario, we designed 2 sets of observation locations, at 50 km and 100 km altitude, observing from a pole direction. Although the component of the impact Delta-V normal to the Didymos system equatorial plane would be practically invisible, this should give near optimal results for the impact geometry planned to date. The observation durations were 4, 12, and 31 days, and included impulse maneuvers every 4 days for orbit maintenance. The uncertainty assumed for those impulse maneuvers are the same as for the DART impact, 1 mm/s; after performing proximity operations in the vicinity of the Didymos system for a few months, this error is reasonable, although arbitrary. The simulated data included both radiometric and optical navigation measurements as in previous sections. We did not compare to a radiometric only data set in this case.

Figures 11 and 12 give a representation of the observation locations at 100 km and 50 km altitude, respectively. Figures 13 and 14 give the ranges to Didymain and Didymoon corresponding to those locations.

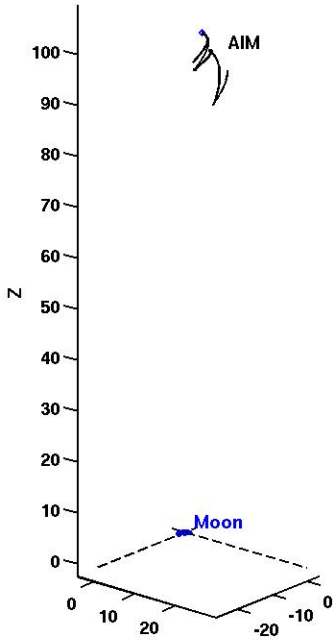

Fig. 11. DART-impact observation location for 100 km altitude.

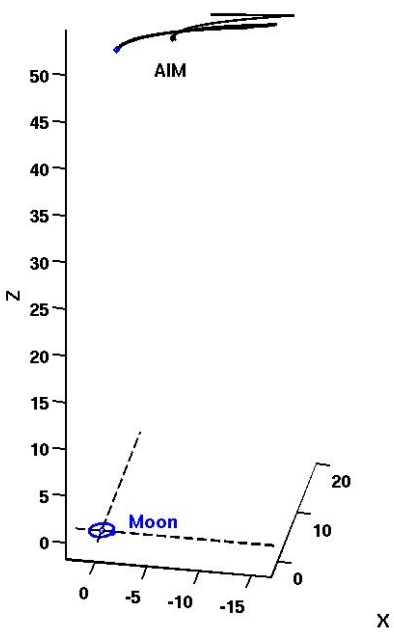

Fig. 12. DART-impact observation location for 50 km altitude.

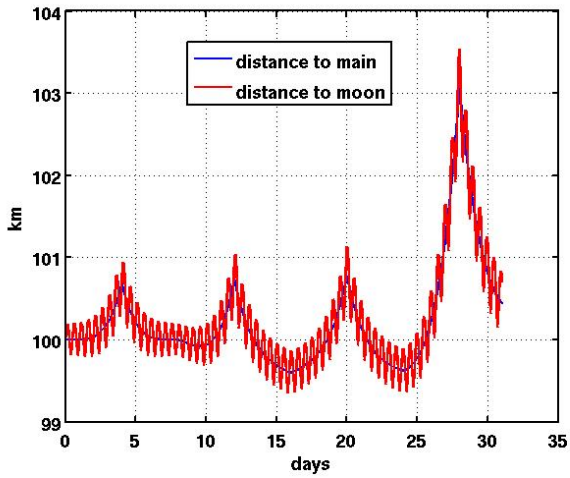

Fig. 13. Range profile for the 100 km observation plateform.

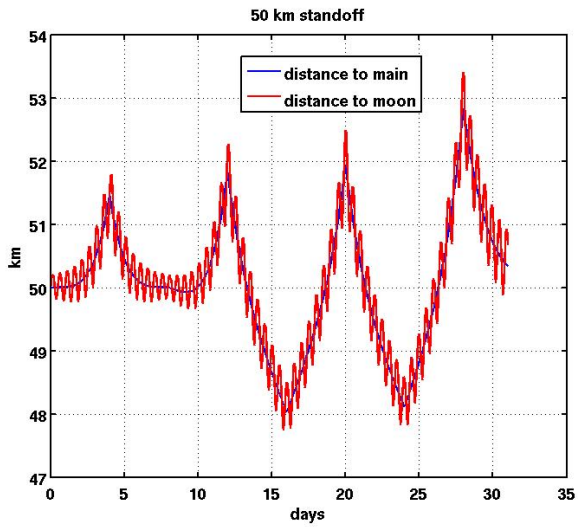

Fig. 14. Range profile for the 50 km observation plateform.

In Figure 15, the uncertainty on the radial and transverse components of the Delta-V is given as function of orbit time. The difference in measurability is especially visible for the radial components; the Delta-V uncertainty drops to 0.3 mm/s in the 50 km case, after 12 days of observation, whereas it stays around 0.5 mm/s for the 100 km case. Both transverse uncertainties drop below 0.1 mm/s after 12 days.

Another parameter of interest is the Beta uncertainty, which correspond to the uncertainty in the transfer of momentum due to the body physical properties. Delta-Beta is calculated by taking the Delta-V uncertainty projected along the surface normal at the impact location, and normalizing by the impact Delta-V magnitude. Figure 16 shows the corresponding Beta uncertainty from the two observation locations. After 12 days of observation, the uncertainty drops below 0.25, which would be sufficient for soil differentiation (see expected Beta values in [4]).

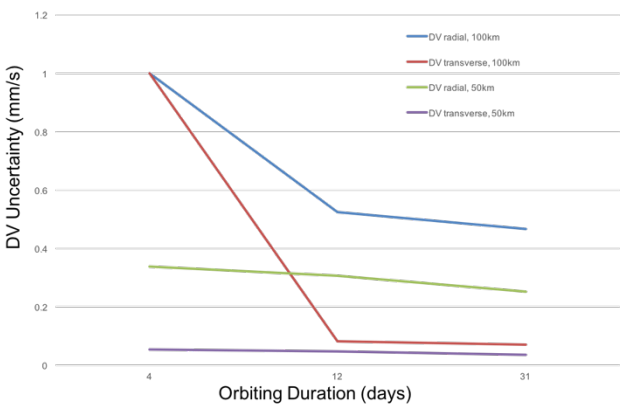

Fig. 15. Delta-V uncertainty as function of orbiting time for both the 100 km and 50 km observation locations, with initial 1-σ uncertainty of 1mm/s.

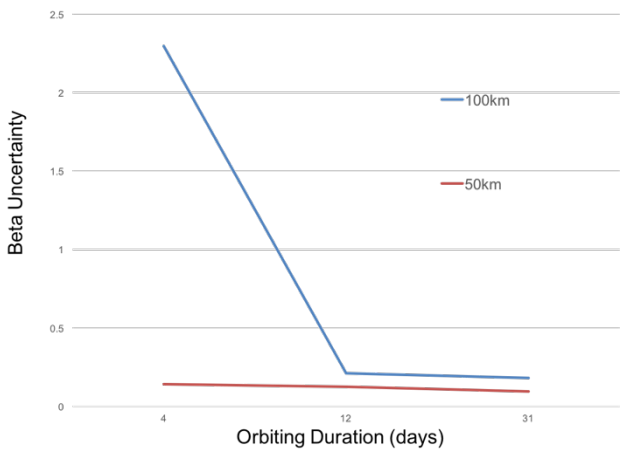

Fig. 16. Beta uncertainty for the 100 km and 50 km observation locations, dropping below 0.25 after 12 days.

6. Conclusion

This paper looks at radio science at the binary asteroid system Didymos in the context of the AIDA mission concept, where the DART spacecraft would be impacting the secondary moon while AIM would be observing. With convential approaches, the GM of the main and moon asteroid can be determined to less than 1% for the main with orbit altitudes below 10 km, and to less than 5% for the moon with orbit altitudes below 4 km.

After the DART impact, Delta-V uncertainty less than 0.1 mm/s could be obtained in the transverse direction when observing from the 50 km polar location for over a week, while the radial component could be measured to less than 0.3 mm/s. At 100 km distance, a DV uncertainty less than 0.1 mm/s and 0.5 mm/s would be achievable over 30 days, for the transverse and radial components, respectively.

Hence, following a radio science campaign with AIM, the improvement in the Didymos system uncertainties allows measurement of the Delta-V imparted by DART when within 50 km altitude. In addition to demonstrating the deflection technique, it is then possible to determine the momentum enhancement, Delta-Beta, which is directly linked to the asteroid porosity.

Acknowledgments

The Cassini mission is operated out of the Jet Propulsion Laboratory, California Institute of Technology, under a contract with the National Aeronautics and Space Administration. @ 2017 California Institute of Technology. Government sponsorship acknowledged.

References

1) Asteroid Impact Mission, ESA website: http://www.esa.int/Our_Activities/Space_Engineering_Technology/Asteroid_Impact_Mission/Asteroid_Impact_Mission2 .
2) P. Michel, A. Cheng, M. Kuppers, P. Pravec, J. Blum, et al.: Science case for the Asteroid Impact Mission (AIM) : A Component of the Asteroid Impact and Deflection Assessment (AIDA) Mission, *Advances in Space Research* 2016, 57, 2529-2547.
3) Double Asteroid Redirection Test: APL website: http://dart.jhuapl.edu/ .
4) A.F. Cheng, J. Atchison, B. Kantsiper, A.S. Rivkin, A. Stickle, C. Reed, A. Galvez, I. Carnelli, et al.: Asteroid Impact and Deflection Assessment Mission, *Acta Astronautica* 2015, 115, 262-269.
5) J.K.Miller, A.S. Konopliv, P.G. Antreasian, D.J. Scheeres: Determination of Shape, Gravity, and Rotational State of Asteroid 433 Eros, *Icarus* 2002, 155(1):3-17.
6) D.K. Yeomans: Comet and Asteroid Ephemerides for Spacecraft Encounter, p1:12, In I.M. Wytrzyszczak et al: Dynamics and Astrometry of Natural and Artificial Celestial Bodies, *Proceedings of IAU Colloquium* 165 Poznań, Poland 1996.
7) M. Yoshikawa et al: The nature of asteroid Itokawa revealed by Hayabusa, Near Earth Objects, our Celestial Neighbors: Opportunity and Risk, *Proceedings of the International Astronomical Union Symposium* 2006, 236.
8) D.J. Scheeres et al.: The Actual Dynamical Environment About Itokawa, *AIAA/AAS Astrodynamics Specialist Conference and Exhibit* 2006, AIAA 2006-6661.
9) M. Patzold et al.: A homogeneous nucleus for comet 67P/Churyumov–Gerasimenko from its gravity field, 2016 Nature 530, 63–65.
10) S. Broschart et al.: Shadow Navigation Support at JPL for the Rosetta Landing on Comet 67P/Churyumov–Gerasimenko, *26th International Symposium on Space Flight Dynamics*, Japan, 2016.
11) Scheeres D.J., *Orbital Motion in Strongly Perturbed Environments*, Springer (2012)
12) JPL Solar System Dynamics Group Horizons web interface: https://ssd.jpl.nasa.gov/horizons.cgi
13) S. Evans et al: MONTE: The Next Generation of Mission Design & Navigation Software, *6th International Conference on Astrodynamics Tools and Techniques (ICATT)*, Germany, 2016.
14) JPL Solar System Dynamics Group Eugene Fahnestock personal communications
15) Didymos Facts and Figures, ESA AIDA reference document: http://www.esa.int/Our_Activities/Space_Engineering_Technology/Asteroid_Impact_Mission/Didymos_facts_figures
16) J. W. McMahon, D. Farnocchia, D. Scheeres, S. Chesley: Understanding Kaula's Rule for Small Bodies, *47th Lunar and Planetary Science Conference* 2016, 2016-2129.